Applied Physics Letters

Cracking behavior in lead zirconate titanate films with different Zr/Ti ratios

Cite as: Appl. Phys. Lett. **121**, 162907 (2022); https://doi.org/10.1063/5.0106340
Submitted: 28 June 2022 • Accepted: 28 September 2022 • Published Online: 20 October 2022

Christopher Cheng, Travis Peters and Susan Trolier-McKinstry

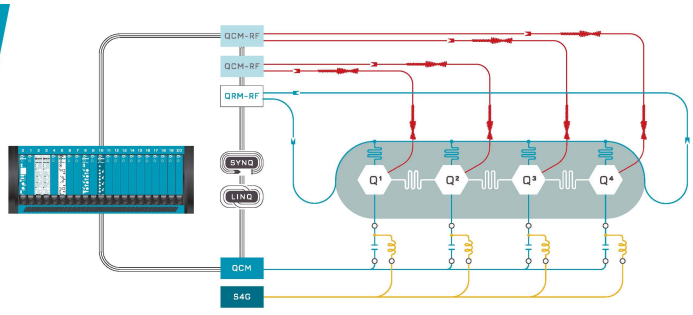

AIP Publishing

Applied Physics Letters ARTICLE scitation.org/journal/apl

Cracking behavior in lead zirconate titanate films with different Zr/Ti ratios

Cite as: Appl. Phys. Lett. **121**, 162907 (2022); doi: 10.1063/5.0106340
Submitted: 28 June 2022 · Accepted: 28 September 2022 ·
Published Online: 20 October 2022

Christopher Cheng,[a] Travis Peters, and Susan Trolier-McKinstry

AFFILIATIONS

Department of Materials Science and Engineering, Pennsylvania State University, University Park, Pennsylvania 16802, USA

Note: This paper is part of the APL Special Collection on Piezoelectric Thin Films for MEMS.
[a]**Author to whom correspondence should be addressed:** set1@psu.edu

ABSTRACT

Crack initiation stresses for different lead zirconate titanate (PZT) film compositions were investigated. PZT/Pt/TiO_2/SiO_2/Si stacks with 2.0 μm thick {100} oriented PZT films at the morphotropic phase boundary (MPB) showed a characteristic strength of 1137 MPa, and the film thickness served as the limiting flaw size for failure of the film/substrate stack. In contrast, for Zr/Ti ratios of 40/60 and 30/70, the characteristic stack strength increased while the Weibull modulus decreased to values typical for that of Si. This difference is believed to be due to toughening from ferroelasticity or phase switching. X-ray diffraction showed that the volume fraction of c-domains increased in Ti-rich compositions. This would allow for more switching from c to a-domains under biaxial tensile stress. Zr/Ti concentration gradients were present for all compositions, which contributed to the observation of a rhombohedral phase off the MPB. Due to the reduced tendency toward cracking, off-MPB compositions are potentially of interest in actuators, albeit with the trade-off of needing a high actuation voltage.

Thin film-based piezoelectric devices are typically driven to high fields and are subject to higher stresses and strains than are bulk ceramics of the same composition. These films often have high levels of residual stresses, which affect both the domain structure and piezoelectric properties.[1–5] Moreover, if the combination of residual stress, applied stress, and piezoelectrically induced stresses exceeds a material-dependent threshold, it can induce cracks or delaminations.[6,7] Film thickness, poling conditions, lead content, crystallographic orientation, temperature, dopants, surface quality, and grain size[8–16] all influence crack formation in PZT films and ceramics. Cracking in piezoelectric films can also induce subsequent thermal dielectric breakdown events, causing failure.[17,18] Thus, the knowledge of the mechanical limits of PZT is required to appropriately design use conditions for the films.

One factor that can influence the propensity for cracking in PZT ceramics is toughening associated with either stress-induced ferroelastic domain reorientation or stress-induced phase changes. PZT ceramics tend to become tougher as cracks elongate—this is known as R-curve behavior. It is reported that stress-induced ferroelastic domain switching is the primary toughening mechanism in PZT ceramics.[15–26] When a crack tip domain is exposed to high mechanical stress under an applied load, the ferroelastic domains reorient to reduce the local stresses.

Ferroelastic toughening is influenced by three material properties: coercive stress, saturated strain, and elastic modulus.[16–27] Of these, the coercive stress has the greatest influence on toughness enhancement, as it determines the process zone size.[19] In principle, ferroelastic toughening should increase with greater lattice distortion (e.g., higher tetragonal PZT distortions) such that a given volume fraction of the domain reorientation would lead to larger compressive stresses on the crack.[14–19] A second reported contribution to toughening is stress-induced phase transformations. During mechanical loading, adjacent grains interact with one another, generating local stresses, which drive transformations between different ferroelectric distortions.[27]

The phenomenon of stress-induced ferroelastic domain switching and phase transformation is well documented in the literature. Zhang *et al.* showed that when PZT ceramics are subjected to high compressive stress, the elastic stiffening behavior differs for PZT-5H, PZT-5A, PTZ-4, and PZT-8. The coercive stresses for soft ceramics were reported to be ~40–50 MPa; for hard ceramics, they were ~60–150 MPa.[28] Seo *et al.* found that the coercive stresses were dependent on the PZT composition with a minimum of ~50 MPa at the MPB and increasing to ~200 MPa at 60% $PbTiO_3$ concentrations.[27] Seo *et al.* further reported that tetragonal PZT ceramics showed lower ferroelastic toughening than rhombohedral compositions.[14]

In particular, increased lattice distortion increased the coercive stress, resulting in fewer switched domains and lower toughening.[14]

Ferroelastic switching and, thus, ferroelastic toughening can be enhanced by either a large c/a ratio (large distortion) and/or a large starting population of c-domains available for switching at the crack tip. This situation is most likely to occur when there is a larger fraction of *c*-domains available in the material. It is well known that the Zr/Ti ratio influences ferroelectric, ferroelastic, and domain populations in films.[29–32] It is likewise known that compressive stress in {100} oriented perovskite films induces *c*-domains, while films under tensile stress induce *a*-domains.[10] Thus, the Zr/Ti content can potentially affect the degree of ferroelastic switching and ferroelastic strengthening.

Finite fracture mechanics describes two conditions that need to be fulfilled for crack initiation in brittle materials such as PZT films.[33–35] First, the tensile stress should be larger than the material tensile strength; second, the increase in the potential energy for finite crack length increase should exceed the material toughness. The energy criterion depends on the stored energy before cracking; as the thickness of the material decreases, more work and energy are needed to create new surfaces. Coleman *et al.* showed that for PZT 52/48 films, the crack initiation stress increased when the film thickness decreased.[17,18] In addition, the characteristic strength of the PZT film/substrate stack decreased with increasing film thickness; it was found that the PZT film thickness functions as the initial crack length that initiates failure of the stack at higher loads.[17,18] Whether this holds true at compositions off the morphotropic phase boundary has not yet been explored.

Additionally, the electrical and mechanical history of PZT affects the propensity of cracking.[17,18,36] Films experience residual thermal stresses from processing, electrically induced stresses from piezoelectric responses, and applied stress from bending. In many films, the residual stress state arises from the PZT film cooling down from the crystallization temperature (T_{cryst}) to the Curie temperature (T_C). The residual thermal stress, σ_t, is associated with the thermal expansion coefficient mismatch between the film and the substrate and can be calculated via

$$\sigma_t = \frac{\int_{T_C}^{T_{cryst}} \left(\alpha_{CTE,f} - \alpha_{CTE,sub}\right) dT}{\left[\left(\frac{1-\nu_f}{Y_f}\right) + \left(\frac{1-\nu_{sub}}{Y_{sub}}\right)\left(4 \cdot \frac{t_f}{t_{sub}}\right)\right]}, \quad (1)$$

where α_{CTE}, ν, and Y are the thermal expansion coefficient, Poisson's ratio, and Young's modulus, respectively.[18,37] The subscripts *f* and *sub* denote the film and substrate, respectively. If the substrate is significantly thicker than the film, Eq. (2) can be simplified to

$$\sigma_t = \left(\frac{Y_f}{1-\nu_f}\right) \int_{T_C}^{T_{crystallization}} \left(\alpha_{CTE,f} - \alpha_{CTE,sub}\right) dT. \quad (2)$$

For PZT, the Curie temperature increases with increasing tetragonality (more $PbTiO_3$).[38,39] Thus, as the film cools from the crystallization temperature to the Curie temperature, the residual film thermal stress induced by processing decreases with increasing tetragonality based on Eqs. (1) and (2). PZT films deposited on SiO_2/Si substrates with less residual thermal tensile stress should be able to withstand higher applied stresses.

This Letter investigates the crack initiation stresses of PZT films at Ti-rich compositions off the morphotropic phase boundary and examines the possible mechanistic contributions that affect the crack behavior of these compositions.

PZT films of 52/48, 40/60, 30/70, and 20/80 compositions were prepared on four-inch Si wafers with ~45 nm TiO_2 and 100 nm of hot sputtered platinum. PZT was prepared and deposited using the inverted mixing order (IMO) solution procedure described elsewhere.[40] The samples were all {001} oriented with a target thickness of 2.0 μm. 100 nm Pt top electrodes were deposited via sputtering and patterned via lift off.

The samples were then diced into 1.2 × 1.2 cm^2 squares, which were placed in the ball-on-3-ball (B3B) measurement setup to evaluate the strength of the entire stack (PZT/Pt/TiO_2/SiO_2/Si) and crack initiation stress in the PZT films, as described by Coleman *et al.*[9,18] A preload of ~10 N was employed to hold the sample between the four balls, and all tests were conducted at room temperature with a compression displacement control of 0.1 mm/min on a universal tester (Instron, MA). At least ten samples were tested to failure per composition to obtain a Weibull analysis on the strength of the sample stack. To investigate crack initiation stresses, the samples were loaded at approximately 30%–95% of the characteristic Weibull strength. Each new load condition required a new sample. (All samples were only loaded once.) Afterwards, the surface of PZT was evaluated for cracks via field emission scanning electron microscopy (FESEM) and dark field optical microscopy. In areas where cracks were suspected, cross sections were prepared via focused-ion-beam (FIB) to inspect if cracks propagated through the PZT film thickness.

The x-ray diffraction (XRD) pattern and field emission scanning electron microscopy (FESEM) images of different compositions are shown in Fig. S1 of the supplementary material. They all had similar Lotgering factors (>95%) and {001} oriented PZT, although a small amount of pyrochlore was present on the surface for the 40/60 and 30/70 compositions. The films were columnar, such that the grains are one grain through the film thickness. The lateral grain sizes were statistically similar for the 52/48 (195 ± 15 nm), 40/60 (186 ± 36 nm), and 30/70 (218 ± 17 nm) compositions. It was found that the microstructure was significantly different for 20/80 PZT compared to the other compositions (126 ± 40 nm). The crystallization temperature of $PbTiO_3$ is lower than $PbZrO_3$. Therefore, when the Zr/Ti ratio increases, the time for PbO loss increases, and vice versa.[41] Excess lead is also known to induce more grain nucleation.[11,12] Thus, the 20/80 composition was excluded for this study.

The Weibull modulus and characteristic strength of the stack were extracted from the B3B data via Weibull analysis using

$$P_f(\sigma) = 1 - \exp\left(-\left(\frac{\sigma}{\sigma_o}\right)^m\right), \quad (3)$$

where $P_f(\sigma)$ is the probability of failure at an applied stress (σ), m is the Weibull modulus, and σ_o is the characteristic Weibull strength (where the probability of failure below this applied stress is 63%).[42,43]

The resultant Weibull modulus and characteristic stack strengths for each composition are given in Fig. 1 and Table I. The MPB composition was found to have a Weibull modulus and a characteristic strength of 11–24 and 1091–1183 MPa, respectively, at a 95% confidence interval. This agrees with previous studies conducted by

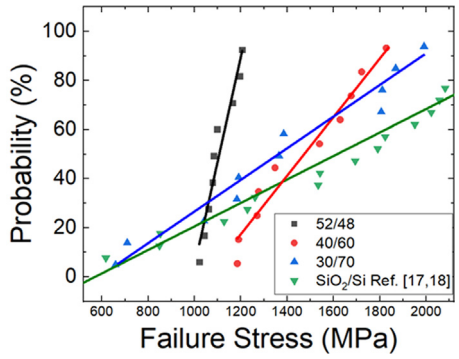

FIG. 1. Probability of failure vs failure stress for 2-μm thick PZT films with different Zr/Ti ratios on Pt/TiO_2/SiO_2/Si substrates using B3B biaxial loading conditions.

Coleman *et al.* showing that MPB PZT films reduce the strength of the entire stack and increase the Weibull modulus compared to that of the Si substrate.[9,18] In this case, the PZT thickness provides a well-defined critical flaw size, resulting in a higher Weibull modulus than that of the substrate.[9,18] The cracks were observed near the midpoint of the sample surface, where the B3B induced the maximum biaxial tensile stress, agreeing with the literature.[9,18]

In contrast, the Weibull modulus for the 40/60 and 30/70 compositions were 4.6–6.2 and 2.5–3.6, respectively, at a 95% confidence interval. This was much lower than the value for the MPB composition. Moreover, the characteristic strength for the 40/60 and 30/70 compositions were 1453–1705 and 1355–1807 MPa, respectively, at a 95% confidence interval. This was similar to the SiO_2/Si substrate (the Weibull modulus and characteristic strengths of 2.3–2.8 and 1647–2126 MPa). That is, as the PZT composition increases in tetragonality, the Weibull moduli and characteristic strength for the entire stack approach the Weibull moduli and the characteristic strength of the SiO_2/Si substrate itself. A low Weibull modulus indicates a wide distribution of critical flaw sizes.[44–47] Thus, the lower Weibull modulus with increasing tetragonal compositions suggests that either (a) the non-MPB PZT films have cracks with a broad distribution of critical flaw sizes, such that the film thickness does not act as a characteristic flaw size, (b) the PZT layer does not crack prior to failure of the SiO_2/Si stack, and/or (c) the small volume fraction of the pyrochlore phase acts to toughen the film. It is believed that this last possibility is less likely, as the volume fraction of pyrochlore was low, as is evidenced by the good orientation through the film; the {100} orientation is typically degraded when extensive pyrochlore is present.[48,49]

To evaluate crack initiation stress, specimens with the 40/60 and 30/70 films were loaded at either ~30% or ~90% of the characteristic Weibull strength. In neither case were cracks discernable on the PZT surface. This contrasts with PZT 52/48 films, where cracks were visible in the electron microscope below the stack strength; these cracks extended through the PZT thickness, were often hundreds of micrometers to mm in length, and served as the flaws that lowered the stack strength and increased the Weibull modulus.[17,18] The absence of observable pre-cracking (and, hence, the absence of a characteristic crack length) in the PZT 40/60 and 30/70 compositions is consistent with the low observed Weibull modulus and the high stack failure strength. Thus, a wide distribution of flaws in the SiO_2/Si substrate governed failure in samples with tetragonal PZT films.

There are at least two mechanisms that might contribute to the reduced observation of cracking in the tetragonal films, relative to the MPB PZT contributions. First, in tetragonal PZT, ferroelastic domain switching between a and c-domains can act to reduce local stresses and so could increase the toughness. To ascertain different domain populations of the films in this study, the {002} XRD peaks of different compositions were analyzed via Pseudo-Voigt peak fitting in LIPRAS software.[50] The best results were achieved when three peaks were fitted (corresponding to a-domain, rhombohedral, and c-domain), as shown in Fig. S2 of the supplementary material. The presence of the rhombohedral phase far from the MPB can arise from composition gradients during the sol-gel deposition process, the influence of film stress, and/or inhomogeneity in the sol-gel solution. For example, Ti-rich conditions at the bottom of the layer led to Zr/Ti gradient formation as $PbTiO_3$-rich compositions provide favorable nucleation in comparison to $PbZrO_3$-rich ones.[12,51,52] Vaxelaire *et al.* found that the crystallographic gradient correlated with Zr/Ti chemical gradients; thus, the entire PZT film may not be at the MPB but can instead alternate between rhombohedral (Zr-rich zones) and tetragonal (Ti-rich zones).[53]

To verify the presence of concentration gradients, scanning transmission electron microscopy (STEM) was used in conjunction with energy-dispersive x-ray spectroscopy (EDS). The samples were prepared creating a cross section with a Helios 660 and a Scios 2 focused ion beam (FIB)/SEM. The ion beam deposition and milling are performed at 30 kV with currents as high as 30 nA for trenching with the exception of the final polishing step at 5 kV. The cross-sectional TEM specimens were observed by the FEI Titan3 G2 double aberration-corrected microscope at 300 kV. The STEM images were collected using a high angle annular dark field (HAADF), which had a collection angle of 52–253 mrad. EDS maps and line scans were collected by using a SuperX EDS system under the STEM mode. The results are shown in Fig. 2. The PZT 52/48 composition had Zr gradients that fluctuated from 45 to 60 mol. % at the 25th and 75th percentile range from the box-and-whisker plots shown in Fig. 2(d); this is comparable

TABLE I. Characteristic load, characteristic strength, and Weibull modulus for Various PZT compositions on the SiO_2/Si substrate and the SiO_2/Si substrate.[17,18] Brackets indicate 95% confidence intervals.

PZT composition	Characteristic load (N)	Characteristic strength (MPa)	Weibull modulus	Time to failure (s)
52/48	130 [125–135]	1137 [1091–1183]	17 [11–24]	62 ± 12
40/60	180 [166–195]	1579 [1453–1705]	6.7 [4.6–8.2]	71 ± 10
30/70	181 [155–207]	1581 [1355–1807]	3.0 [2.5–3.6]	75 ± 31
SiO_2/Si	216 [189–244]	1887 [1647–2126]	2.5 [2.3–2.8]	N/A

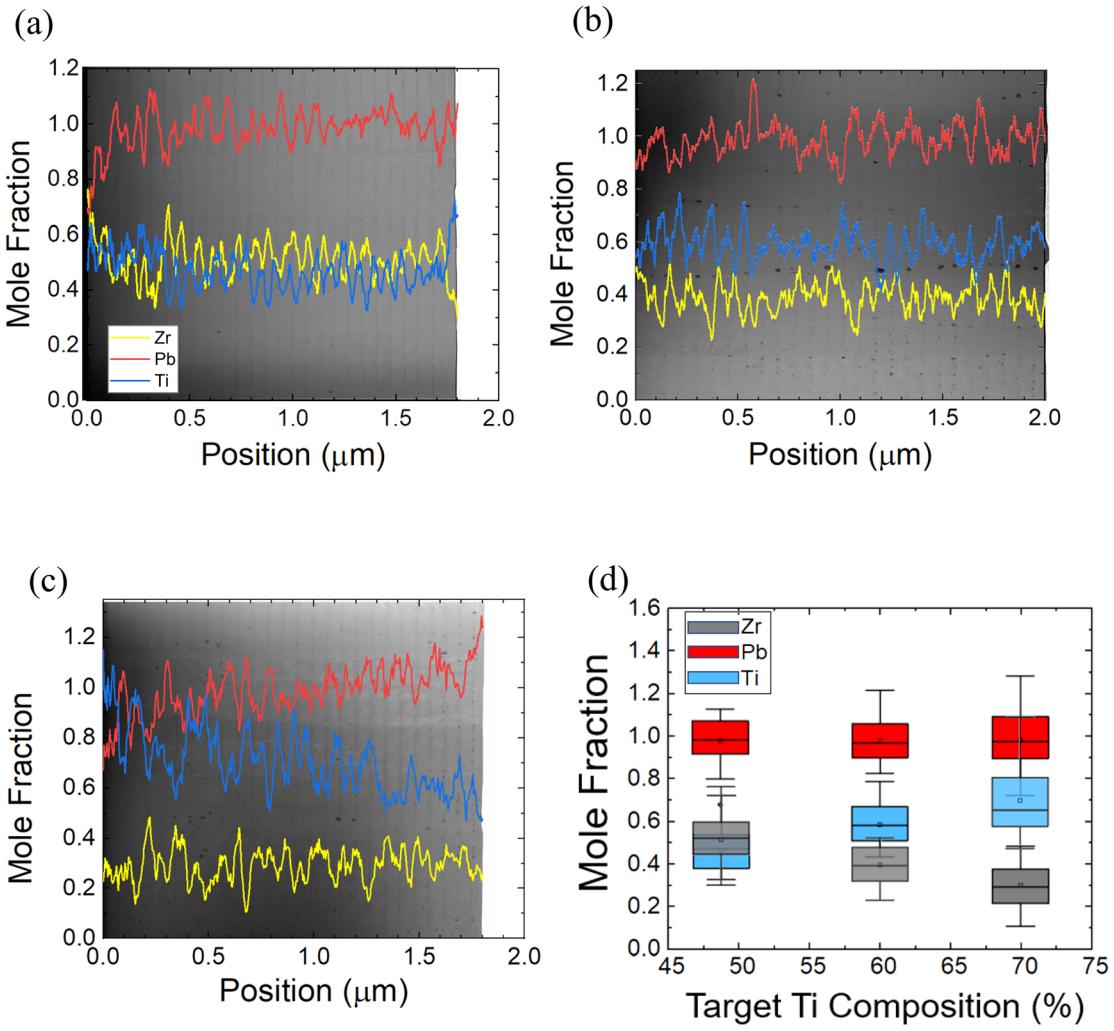

FIG. 2. TEM line scans of PZT compositions: (a) 52/48, (b) 40/60, and (c) 30/70. The films were acquired such that the position is perpendicular to the substrate. Position 0 is the film surface. The extrema correspond to each of the crystallization layers with high Ti and Pb concentrations near the bottom of each crystallized layer and high Zr contents at the top of each crystallized layer. (d) Box-and-whisker plots of the gradients of Zr, Pb, and Ti for each composition.

to reported composition fluctuations in other PZT sol gel solutions on $Pt/TiO_2/SiO_2/Si$ substrates.[52,54] The interquartile range for the mole fraction Zr was similar for all compositions 16.1, 16.1, and 15.2 mol. % for 30/70, 40/60, and 52/48 compositions, respectively. The interquartile range for the mole fraction of Pb was also similar for all compositions (20, 16, and 16 mol. % for 30/70, 40/60, and 52/48 compositions, respectively). The interquartile range for the mole fraction of Ti for 30/70, 40/60, and 52/48 was 23.0, 15.8, and 15.7 mol. %, respectively. It is believed that one cause of the observed rhombohedral phase is these concentration gradients. The presence of mechanical strains, local strains, or a shift in the MPB due to non-stoichiometry and the presence of lead on the B-site[55,56] are additional factors that could induce a rhombohedral phase off the MPB.

The lattice parameters and area underneath the fitted peaks were extracted from the Pseudo-Voigt fits via MatLab and are given in Table S1 with Fig. S3 of the supplementary material comparing the extracted lattice parameters to those reported by Shirane and Suzuki.[57] When the average film compositions were more Ti-rich, the rhombohedral phase fraction decreased and the a-domain volume fraction increased. Furthermore, the concentration of c-domains increased with increasing tetragonality. It is noted that the compositional gradients will presumably also introduce strain gradients. The role of these gradients are cracking is unknown and difficult to quantify, as such gradients may also influence the local domain structure.

The second potential contribution to a higher characteristic strength for tetragonal films is that they have slightly lower residual stresses than MPB films and can, thus, withstand higher loading stresses, increasing their characteristic strength. To estimate the biaxial residual thermal stress, phenomenological parameters were inserted into Eq. (1); the data used in the calculations are given in Table S2 of the supplementary material. It was found that the thermal stresses in the film are tensile for films on Si substrates and did not significantly

vary between compositions based on phenomenological calculations; the thermal stresses were 82.0, 87.2, and 79.9 MPa for the 52/48, 40/60, and 30/70 compositions, respectively. It should be noted that this calculation only addresses the thermal strain on cooling from the crystallization temperature to T_C and does not account for any stress relaxation associated with development of the domain state on cooling through T_C. In addition, there are numerous papers showing reasonable agreement between calculated thermal stresses and stresses measured via wafer bowing experiments.[5,58–60]

In conclusion, {100} oriented PZT films with Zr/Ti ratios of 52/48, 40/60, 30/70, and 20/80 were fabricated via the IMO sol-gel method to investigate their respective cracking behaviors. The PZT 52/48 behavior was in good agreement with the work by Coleman *et al.*[9] However, for more tetragonal films, the characteristic strength increased while the Weibull modulus decreased to values comparable to that of the Si substrate. The residual thermal tensile stress accumulated due to the thermal expansion differences did not significantly vary between average 52/48 and 30/70 compositions; it is unknown if there was a difference in the relaxation of the stresses due to domain formation below the Curie temperature. Thus, it is speculated that the higher stack strengths are associated with increased toughening due to either ferroelastic switching or phase switching in samples with more Ti-rich PZT. Based on peak fitting, the PZT films had a mixture of the tetragonal a-domain, tetragonal c-domain, and rhombohedral phases for all compositions; the rhombohedral phase decreased while both tetragonal a and c-domain fractions increased with increasing tetragonality. TEM confirmed the existence of Zr/Ti concentration gradients in all films. This likely accounts for the rhombohedral peak found in the XRD peak fitting.

Future experiments should include local *in situ* XRD measurements of the PZT films pre- and post-cracking to ascertain a change in the crystal structure from the initial state. It is noted that ferroelastic domain switching is widely reported to be modest in clamped PZT films on a silicon substrate,[5,61–65] so that it is anticipated that relatively small macroscopic changes in the domain state will occur over large process zones. Local measurements would allow this hypothesis to be checked as well as allow the determination of the zone of ferroelastic switching around a crack front to be determined.

From an acoustic device perspective, the maximum displacement is desired for acoustic sources. To maximize the displacement, a maximum lateral strain or applied electric field is needed. In scenarios where the PZT compositions do not crack, PZT 52/48 would be ideal due to its large piezoelectric coefficient. Practically, however, the PZT samples do crack in some device configurations (e.g., depending on the release state, clamping conditions, and PZT film thickness). Thus, off-MPB compositions are potentially of interest in actuators due to the reduced propensity for cracking, albeit with a trade-off associated with the need to apply higher electric fields.

See the supplementary material for XRD/FESEM characterization of the grown films, pseudo-Voigt fits using LIPRAS software and its resultant 2Θ positions and area under the fitted curves, and finally, the mechanical properties used for estimating residual thermal stress in Eq. (1).

The authors would like to thank Trevor Clark and Ke Wang for their help on TEM sample preparation and imaging.

AUTHOR DECLARATIONS

Conflict of Interest

The authors have no conflicts to disclose.

Author Contributions

Christopher Cheng: Conceptualization (lead); Data curation (lead); Formal analysis (lead); Investigation (lead); Methodology (lead); Resources (lead); Validation (lead); Writing – original draft (lead). **T. Peters:** Resources (supporting); Writing – review & editing (supporting). **S. Trolier-McKinstry:** Funding acquisition (lead); Resources (equal); Supervision (lead); Writing – review & editing (equal).

DATA AVAILABILITY

The data that support the findings of this study are available within the article and its supplementary material. The data that support the findings of this study are available from the corresponding author upon reasonable request due to restrictions.

REFERENCES

[1]M. Okayasu, Y. Sato, M. Mizuno, and T. Shiraishi, "Mechanically controlled domain structure in PZT piezoelectric ceramics," Ceram. Int. **38**(6), 4579–4585 (2012).
[2]K. Lefki and G. J. M. Dormans, "Measurement of piezoelectric coefficients of ferroelectric thin films," J. Appl. Phys. **76**(3), 1764 (1994).
[3]H. G. Yeo and S. Trolier-McKinstry, "{001} Oriented piezoelectric films prepared by chemical solution deposition on Ni foils," J. Appl. Phys. **116**(1), 014105 (2014).
[4]B. Ma, S. Liu, S. Tong, M. Narayanan, and U. Balachandran, "Enhanced dielectric properties of $Pb_{0.92}La_{0.08}Zr_{0.52}Ti_{0.48}O_3$ films with compressive stress," J. Appl. Phys. **112**(11), 114117 (2012).
[5]K. Coleman, J. Walker, T. Beechem, and S. Trolier-McKinstry, "Effect of stresses on dielectric and piezoelectric properties of $Pb(Zr_{0.52}Ti_{0.48})O_3$ thin films," J. Appl. Phys. **126**(3), 034101 (2019).
[6]B. Audoly, "Stability of straight delamination blisters," Phys. Rev. Lett. **83**(20), 4124–4127 (1999).
[7]A. Lee, B. M. Clemens, and W. D. Nix, "Stress induced delamination methods for the study of adhesion of Pt thin films to Si," Acta Mater. **52**(7), 2081–2093 (2004).
[8]Z. Zhang and R. Raj, "Influence of grain size on ferroelastic toughening and piezoelectric behavior of lead zirconate titanate," J. Am. Ceram. Soc. **78**(12), 3364–3368 (1994).
[9]K. Coleman, R. Bermejo, D. Leguillon, and S. Trolier-McKinstry, "Thickness dependence of crack initiation and propagation in stacks for piezoelectric microelectromechanical systems," Acta Mater. **191**, 245–252 (2020).
[10]A. Mazzalai, D. Balma, N. Chidambaram, P. Muralt, L. Colombo, and T. Schmitz-Kempen, "Dynamic and long-time tests of the transverse piezoelectric coefficient in PZT thin films," in *Proceedings of IEEE International Symposium on Applications of Ferroelectrics*, *State College, USA* (IEEE, 2014), pp. 1–4.
[11]W. Zhu, T. Borman, K. Decesaris, B. Truong, M. M. Lieu, S. W. Ko, P. Mardilovich, and S. Trolier-McKinstry, "Influence of PbO content on the dielectric failure of Nb-doped {100}-oriented lead zirconate titanate films," J. Am. Ceram. Soc. **102**(4), 1734–1740 (2019).
[12]T. M. Borman, "{001} textured growth of doped, gradient free lead zirconate titanate thin films by chemical solution deposition," M.S. thesis (Department of Materials Science and Engineering, The Pennsylvania State University, University Park, 2016).
[13]Z. Luo, S. Pojprapai, J. Glaum, and M. Hoffman, "Electrical fatigue-induced cracking in lead zirconate titanate piezoelectric ceramic and its influence quantitatively analyzed by refatigue method," J. Am. Ceram. Soc. **95**(8), 2593–2600 (2012).

[14]Y. H. Seo, M. Vogler, D. Isaia, E. Aulbach, J. Rodel, and K. G. Webber, "Temperature-dependent R-curve behavior of $Pb(Zr_{1-x}Ti_x)O_3$," Acta Mater. **61**(17), 6418–6427 (2013).
[15]M. J. Reece and F. Guiu, "Toughening produced by crack-tip-stress-induced domain reorientation in ferroelectric and/or ferroelastic materials," Philos. Mag. A **82**(1), 29–38 (2001).
[16]A. Hizebry, M. Saadaoui, H. Elattaoui, J. Chevalier, and G. Fantozzi, "R-curve and subcritical crack growth in lead zirconate titanate ceramics," Mater. Sci. Eng.: A **499**(1–2), 368–373 (2009).
[17]K. Coleman, J. Walker, W. Zhu, S. W. Ko, P. Mardilovich, and S. Trolier-McKinstry, "Failure mechanisms of lead zirconate titanate thin films during electromechanical loading," in *Proceedings of Joint Conference of the IEEE IFCS-ISAF, Keystone, CO, USA* (IEEE, 2020), pp. 1–5.
[18]K. Coleman, "Influence of stress on the performance of lead zirconate titanate thin films," Ph.D. thesis (Department of Materials Science and Engineering, The Pennsylvania State University, University Park, 2020).
[19]Y. H. Seo, A. Bencan, J. Koruza, B. Malic, M. Kosec, and K. G. Webber, "Compositional dependence of R-curve behavior in soft $Pb(Zr_{1-x}Ti_x)O_3$ ceramics," J. Am. Ceram. Soc. **94**(12), 4419–4425 (2011).
[20]F. Meschke, O. Raddatz, A. Kolleck, and G. A. Schneider, "R-curve behavior and crack-closure stresses in barium titanate and (Mg,Y)-PSZ ceramics," J. Am. Ceram. Soc. **83**(2), 353–361 (2000).
[21]A. Kolleck, G. A. Schneider, and F. A. Meschke, "R-curve behavior of $BaTiO_3$- and PZT ceramics under the influence of an electric field applied parallel to the crack front," Acta Mater. **48**, 4099–4113 (2000).
[22]A. B. Kounga Njiwa, E. Aulbach, J. Rödel, S. L. Turner, T. P. Comyn, and A. J. Bell, "Ferroelasticity and R-curve behavior in $BiFeO_3$–$PbTiO_3$," J. Am. Ceram. Soc. **89**(5), 1761–1763 (2006).
[23]A. Ricoeur and M. Kuna, "A micromechanical model for the fracture process zone in ferroelectrics," Comput. Mater. Sci. **27**(3), 235–249 (2003).
[24]M. J. Reece and F. Guiu, "Estimation of toughening produced by ferro-electric/ferroelastic domain switching," J. Eur. Ceram. Soc. **21**(10), 1433–1436 (2001).
[25]Y. Cui and W. Yang, "Toughening under non-uniform ferro-elastic domain switching," Int. J. Solids Struct. **43**(14), 4452–4464 (2006).
[26]C. M. Landis, "On the fracture toughness of ferroelastic materials," J. Mech. Phys. Solids **51**(8), 1347–1369 (2003).
[27]Y. Seo, D. J. Franzbach, J. Koruza, A. Bencan, B. Malic, M. Kosec, J. L. Jones, and K. G. Webber, "Nonlinear stress-strain behavior and stress-induced phase transitions in soft $Pb(Zr_{1-x}Ti_x)O_3$ at the morphotropic phase boundary," Phys. Rev. B **87**, 094116 (2013).
[28]Q. M. Zhang, J. Zhao, K. Uchino, and J. Zheng, "Change of the weak-field properties of $Pb(ZrTi)O_3$ piezoceramics with compressive uniaxial stresses and its links to the effect of dopants on the stability of the polarizations in the materials," J. Mater. Res. **12**(1), 226–234 (1997).
[29]H. Morioka, S. Yokoyama, T. Oikawa, and H. Funakubo, "Spontaneous polarization change with Zr/(Zr+Ti) ratios in perfectly polar-axis-orientated epitaxial tetragonal $Pb(Zr,Ti)O_3$ films," Appl. Phys. Lett. **85**(16), 3516 (2004).
[30]M. J. Hoffmann, M. Hammer, A. Endriss, and D. C. Lupascu, "Correlation between microstructure, strain behavior, and acoustic emission of soft PZT ceramics," Acta Mater. **49**(7), 1301–1310 (2001).
[31]C. Yeager, "PZT thin films for piezoelectric MEMS mechanical energy harvesting," Ph.D. thesis (Department of Materials Science and Engineering, The Pennsylvania State University, University Park, 2015).
[32]S. Hiboux, P. Muralt, and T. Maeder, "Domain and lattice contributions to dielectric and piezoelectric properties of $Pb(Zr_x, Ti_{1-x})O_3$ thin films as a function of composition," J. Mater. Res. **14**, 4307–4318 (1999).
[33]D. Leguillon, "Strength or toughness? A criterion for crack onset at a notch," Eur. J. Mech.—A/Solids **21**(1), 61–72 (2002).
[34]D. Taylor, "The theory of critical distances," Eng. Fract. Mech. **75**(7), 1696–1705 (2008).
[35]D. Leguillon, E. Martin, and M. Lafarie-Frenot, "Flexural vs tensile strength in brittle materials," C. R. Méc. **343**(4), 275–281 (2015).
[36]K. Coleman, M. Ritter, R. Bermejo, and S. Trolier-McKinstry, "Mechanical failure dependence on the electrical history of lead zirconate titanate thin films," J. Eur. Ceram. Soc. **41**(4), 2465–2471 (2021).
[37]M. Ohring, "Mechanical properties of thin films," in *Materials Science of Thin Films Deposition and Structure* (Academic Press, Inc., San Diego, 2002).
[38]M. J. Haun, E. Furman, S. J. Jang, and L. E. Cross, "Thermodynamic theory of the lead zirconate-titanate solution system, part V: Theoretical calculations," Ferroelectrics **99**(1), 63–86 (1988).
[39]M. J. Haun, Z. Q. Zhuang, E. Furman, S. J. Jang, and L. E. Cross, "Thermodynamic theory of the lead zirconate-titanate solution system, part III: Curie constant and sixth-order polarization interaction dielectric stiffness coefficients," Ferroelectrics **99**(1), 45–54 (1988).
[40]T. Peters, C. Cheng, G. A. Rossetti, Jr., and S. Trolier-McKinstry, J. Am. Ceram. Soc. **105**(6), 4058–4070 (2022).
[41]E. F. Alberta, R. Guo, and A. S. Bhalla, "Structure–property diagrams of ferroic solid solutions. Part I: Perovskite relaxor ferroelectrics with morphotropic phase boundaries," Ferroelectr. Rev. **4**, 1–327 (2001).
[42]J. B. Wachtman, W. R. Cannon, and M. J. Mathewson, "Statistical treatment of strength," in *Mechanical Properties of Ceramics* (John Wiley & Sons Inc., Hoboken, 2009), pp. 119–149.
[43]W. Weibull and Kungl Tekniska Högskolan, "A Statistical Theory of the Strength of materials," Ph.D. Thesis (Royal Technical University, Stockholm, Sweden, 1939).
[44]K. S. Chen, A. Ayon, and S. M. Spearing, "Controlling and testing the fracture strength of silicon on the mesoscale," J. Am. Ceram. Soc. **83**(6), 1476–1484 (2004).
[45]C. Funke, E. Kullig, M. Kuna, and H. J. Möller, "Biaxial fracture test of silicon wafers," Adv. Eng. Mater. **6**(7), 594–598 (2004).
[46]D. H. Alsem, B. L. Boyce, E. A. Stach, and R. O. Ritchie, "Effect of post-release sidewall morphology on the fracture and fatigue properties of polycrystalline silicon structural films," Sens. Actuators, A **147**(2), 553–560 (2008).
[47]I. Chasiotis and W. G. Knauss, "The mechanical strength of polysilicon films: Part 1. The influence of fabrication governed surface conditions," J. Mech. Phys. Solids **51**(8), 1533–1550 (2003).
[48]T. Borman, S. W. Ko, P. Mardilovich, and S. Trolier-McKinstry, "Development of crystallographic texture in chemical solution deposited lead zirconate titanate seed layers," J. Am. Ceram. Soc. **100**(10), 4476–4482 (2017).
[49]T. Borman, W. Zhu, K. Wang, S. W. Ko, P. Mardilovich, and S. Trolier-McKinstry, "Effect of lead content on the performance of niobium-doped {100} textured lead zirconate titanate films," J. Am. Ceram. Soc. **100**(8), 3558–3567 (2017).
[50]G. Esteves, K. Ramos, C. M. Fancher, and J. L. Jones, *LIPRAS: Line-Profile Analysis Software* (North Carolina State University, 2017).
[51]P. Muralt, "Texture control and seeded nucleation of nanosize structures of ferroelectric thin films," J. Appl. Phys. **100**(5), 051605 (2006).
[52]F. Calame and P. Muralt, "Growth and properties of gradient free sol-gel lead zirconate titanate thin films," Appl. Phys. Lett. **90**(6), 062907 (2007).
[53]N. Vaxelaire, V. Kovacova, A. Bernasconi, G. L. Rhun, M. Alvarez-Murga, G. B. M. Vaughan, E. Defay, and P. Gergaud, "Effect of structural in-depth heterogeneities on electrical properties of $Pb(Zr_{0.52}Ti_{0.48})O_3$ thin films as revealed by nano-beam x-ray diffraction," J. Appl. Phys. **120**(10), 104101 (2016).
[54]J. F. Ihlefeld, P. G. Kotula, B. D. Gauntt, D. V. Gough, G. L. Brennecka, P. Lu, and E. D. Spoerke, "Solution chemistry, substrate, and processing effects on chemical homogeneity in lead zirconate titanate thin films," J. Am. Ceram. Soc. **98**(7), 2028–2048 (2015).
[55]P. Muralt, S. Hiboux, C. Mueller, T. Maeder, L. Sagalowicz, T. Egami, and N. Setter, "Excess lead in the perovskite lattice of PZT thin films made by in-situ reactive sputtering," Integr. Ferroelectr. **36**(1–4), 53–62 (2001).
[56]V. Kovacova, "Study of correlations between microstructure and piezoelectric properties of PZT thin films," Ph.D. thesis (Université Grenoble Alpes, 2015).
[57]G. Shirane and K. Suzuki, "Crystal structure of $Pb(Zr\text{-}Ti)O_3$," J. Phys. Soc. Jpn. **7**(3), 333 (1952).
[58]B. Tuttle, J. Voigt, T. J. Garino, D. C. Goodnow, R. W. Schwartz, D. L. Lamppa, T. Headley, and M. Eatough, "Chemically prepared $Pb(Zr,Ti)O_3$ thin films: The effects of orientation and stress," in *ISAF 1992: Proceedings of the Eighth IEEE International Symposium on Applications of Ferroelectrics* (IEEE, 1992), pp. 344–348.
[59]M. Eatough, D. Dimos, B. A. Tuttle, W. L. Warren, and R. Bank, "A study of switching behavior in Pb (Zr, Ti)O_3 thin films using x-ray diffraction," Mater. Res. Soc. Symp. Proc. **361**, 111–116 (1994).
[60]B. A. Tuttle and R. W. Schwartz, "Solution deposition of ferroelectric thin films," MRS Bull. **21**, 49–54 (1996).
[61]F. Xu, S. Trolier-McKinstry, W. Ren, B. M. Xu, Z. L. Xie, and K. L. Hemker, "Domain wall motion and its contribution to the dielectric and piezoelectric

properties of lead zirconate titanate films," J. Appl. Phys. **89**(2), 1336–1348 (2001).
[62]N. Bassiri Gharb, I. Fujii, E. Hong, S. Trolier-McKinstry, D. V. Taylor, and D. Damjanovic, "Domain wall contributions to the properties of piezoelectric thin films," J. Electroceram. **19**, 47–65 (2007).
[63]M. Wallace, R. L. Johnson-Wilke, G. Esteves, C. M. Fancher, R. H. T. Wilke, J. L. Jones, and S. Trolier-McKinstry, "*In situ* measurement of increased ferroelectric/ferroelastic domain wall motion in declamped tetragonal lead zirconate titanate thin films," J. Appl. Phys. **117**(5), 054103 (2015).
[64]R. L. Johnson-Wilke, R. H. T. Wilke, M. Wallace, A. Rajashekhar, G. Esteves, Z. Merritt, J. L. Jones, and S. Trolier-McKinstry, "Ferroelectric/ferroelastic domain wall motion in dense and porous tetragonal lead zirconate titanate films," IEEE Trans. Ultrason. Ferroelectr. Freq. Control **62**(1), 46–55 (2015).
[65]L. Denis-Rotella, G. Esteves, J. Walker, H. Zhou, J. Jones, and S. Trolier-McKinstry, "Residual stress and ferroelastic domain reorientation in declamped {001} $PbZr_{0.3}Ti_{0.7}O_3$ films," IEEE Trans. Ultrason. Ferroelectr. Freq. Control **68**(2), 259–272 (2020).